Biomedical Signal Processing and Control 14 (2014) 189–196

Contents lists available at ScienceDirect

Biomedical Signal Processing and Control

journal homepage: www.elsevier.com/locate/bspc

Detection of body position changes from the ECG using a Laplacian noise model

Ana Mincholé [a,*], Leif Sörnmo [b], Pablo Laguna [c]

[a] Department of Computer Science, University of Oxford, UK
[b] Department of Electrical and Information Technology and Center for Integrative Electrocardiology, Lund University, Sweden
[c] CIBER de Bioingeniería, Biomateriales y Nanomedicina (CIBER-BBN), Spain, and the Communications Technology Group (GTC) at the Aragón Institute of Engineering Research (I3A), University of Zaragoza, Spain

ARTICLE INFO

Article history:
Received 4 March 2014
Received in revised form 1 July 2014
Accepted 4 August 2014

Keywords:
Postural changes
Laplacian noise
Detection theory
Ischemia detection

ABSTRACT

Body position changes (BPCs) are manifested as shifts in the electrical axis of the heart, which may lead to ST changes in the ECG, misclassified as ischemic events. This paper presents a novel BPC detector based on a Laplacian noise model. It is assumed that a BPC can be modelled as a step-like change in the two coefficient series that result from the Karhunen–Loève transform of the QRS complex and the ST–T segment. The generalized likelihood ratio test is explored for detection, where the statistical parameters of the Laplacian model are subject to estimation. Two databases are studied: one for assessing detection performance in healthy subjects who perform BPCs, and another for assessing the false alarm rate in ECGs recorded during percutaneous transluminal coronary angiography. The resulting probability of detection (P_D) and probability of false alarm (P_F) are 0.94 and 0.00, respectively, whereas the false alarm rate in ischemic recordings is 1 event/h. The proposed detector outperforms an existing detector based on the Gaussian noise model which achieved a P_D/P_F of 0.90/0.01 and a false alarm rate of 2 events/h. Analysis of the log-likelihood function for the Gaussian and Laplacian noise models show that latter model is more adequate.

1. Introduction

A change in body position causes a change in the position of the heart, manifested in the ECG as a change in morphology of the QRS complex and the ST–T segment [1,2]. Such changes are particularly problematic in ambulatory ST monitoring since they may cause false ischemia alarms [3]. Hence, it is important to develop techniques which discriminate body position changes (BPCs) from true ischemic episodes. Such techniques will not only improve the reliability of ST monitoring, but they will also be useful in polysomnographic signal analysis where a BPC may be misclassified as an apneic event [4].

An early attempt to address the BPC problem was based on the Karhunen–Lòeve transform (KLT) and the pattern of coefficients in the KLT domain, defined both for the QRS complex and the ST–T segment [5]. Based on the assumption that the QRS-related coefficients change more rapidly during a BPC than during an ischemic episode, the results suggested that ischemic episodes can be distinguished from non-ischemic ones in the European ST–T Database. However, detection performance was not explicitly evaluated since BPCs were not annotated [5].

More recently, another KLT-based approach has been proposed and evaluated for detecting BPCs [6]. At the same time, a novel approach was proposed that explores changes in the orientation of the heart's electrical axis as reflected by the rotation angles of the vectorcardiographic loop [7]. For both approaches, a Bayesian-type detector was developed based on the assumption that a BPC is manifested as a step change in Gaussian noise [6,7], see also [8]. The input signal to the detector was a time series defined either by KLT coefficients or rotation angles. The results indicated that both approaches performed relatively well, but signal segments with impulsive noise, baseline wander, and ectopic beats were all found to impair performance and produced high false alarm rates. In such noisy situations, it is advisable to replace the Gaussian noise model with another that better accounts for outlier samples.

A Laplacian noise model has been successfully employed in other biomedical applications [9–13], and is therefore investigated in the present paper for BPC detection. The main novelty is the development of the generalized likelihood ratio test (GLRT) for this particular model. The GLRT involves an alternating optimization

* Corresponding author.
E-mail address: minchole@unizar.es (A. Mincholé).

http://dx.doi.org/10.1016/j.bspc.2014.08.002
1746-8094/

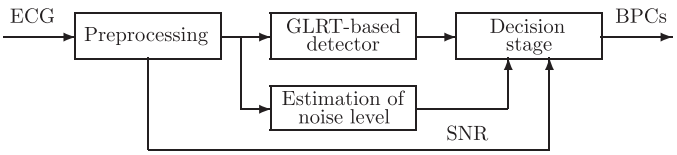

Fig. 1. Block diagram of the proposed BPC detector.

procedure for estimating interdependent statistical parameters. Since the noise level of the observations may change considerably from one patient to another, the standard deviation of the noise model is treated as an unknown parameter which is subjected to maximum likelihood (ML) estimation.

The paper is organized as follows. Section 2 describes the model-based approach to BPC detection. The performance is assessed on two different databases: one with healthy subjects performing BPCs, and another with patients undergoing percutaneous transluminal coronary angiography (PTCA), see Section 3. In Section 5, the performance is compared to that of the Bayesian detector based on the Gaussian model [6]. The paper concludes with a discussion in Section 6.

2. Methods

The proposed BPC detector comprises the steps displayed in Fig. 1, and is described in the following.

2.1. Preprocessing

The preprocessing employed here is similar to the one employed in our previous studies on BPC detection [6,7], and is therefore only briefly summarized. The original 12-lead ECG is transformed into a vectorcardiogram (VCG) by the inverse Dower matrix [14], serving as the basis for subsequent processing. A beat is rejected if its signal-to-noise ratio (SNR) is below either a fixed threshold or a relative threshold defined by a running SNR estimate. The latter threshold ensures that shorter noise periods are rejected, while still allowing for detection of BPCs. The SNR is defined as the ratio between the peak-to-peak QRS amplitude and the RMS value of the high-frequency noise (above 25 Hz) in intervals adjacent to the QRS. The running estimate is determined by exponential averaging, with a forgetting factor of 0.02.

The lengths of the QRS interval and the ST–T segment are set to 130 and 600 ms, respectively. The QRS interval is centred around a fiducial point, whereas the ST–T segment starts at a time that depends on heart rate [15]; ST–T segments shorter than 600 ms are extended by appending zeros [16].

The BPC detector operates in the KLT domain, and uses separate bases for the QRS complex and the ST–T segment. The two bases are derived from about 200 000 waveforms, see [17] for details on the dataset. The function $\varphi_l[n]$, measuring the distance between the KLT coefficient series and related means, defines the input to the BPC detector:

$$\varphi_l[n] = \left(\frac{1}{\overline{E}_l} \sum_{k=1}^{K} \left(\alpha_{l,k}[n] - \overline{\alpha}_{l,k} \right)^2 \right)^{1/2}, \quad l = 1, \ldots, L, \tag{1}$$

where K denotes the maximum order of the KLT coefficients, $\alpha_{l,k}[n]$ the kth order KLT coefficient of the l^{th} lead, $\overline{\alpha}_{l,k}$ the reference mean, and L the number of leads. The function $\varphi_l[n]$ is subject to resampling and normalization by the energy $\overline{E}_l$ of each complex/segment; resampling produces a regularly sampled series with a rate of 1 Hz. Both $\overline{\alpha}_{l,k}$ and $\overline{E}_l$ are computed from the first 50 beats of the analyzed recording [6].

2.2. Signal model

The statistical signal model, previously proposed in [6,7] for the purpose of detecting whether a BPC has occurred (hypothesis $\mathcal{H}_1$) or not (hypothesis $\mathcal{H}_0$), is here further developed. The observation interval is sliding, with its onset at $n = n_0$. A BPC is characterized by a signature waveform $s(n)$, scaled by a lead-dependent amplitude a_l and corrupted by additive, lead-dependent noise $w_l[n]$,

$$\mathcal{H}_0 : \varphi_l[n] = w_l[n], \tag{2}$$

$$\mathcal{H}_1 : \varphi_l[n] = a_l[n_0] s[n - n_0] + w_l[n], \tag{3}$$

where $n = n_0, \ldots, n_0 + N - 1$, $n_0 = 0, \ldots$, and N is an even-valued integer. Body position changes are here modeled by a step function,

$$s[n] = \begin{cases} 1 & n = 0, \ldots, \dfrac{N}{2} - 1, \\ -1 & n = \dfrac{N}{2}, \ldots, N - 1. \end{cases} \tag{4}$$

In contrast to [6,7], the present model formulation circumvents the inclusion of an unknown occurrence time of each observation interval since $s(n)$ extends over the entire observation interval of length N.

The noise $w_l[n]$ is characterized by independent, random variables with a Laplacian probability density function (PDF),

$$p(w_l[n]) = \frac{1}{\sqrt{2}\sigma_l} \exp\left[-\frac{\sqrt{2}}{\sigma_l} |w_l[n] - m_l[n_0]| \right], \tag{5}$$

where $n = n_0, \ldots, n_0 + N - 1$. The statistical parameters $m_l[n_0]$ and σ_l denote the mean and standard deviation of $w_l[n]$, respectively. The noise model in (5) is adopted in the present study because BPC-free data in the KLT domain are better characterized by a Laplacian than by a Gaussian PDF, see Section 5.

2.3. GLRT-based detection

The GLRT is considered since the parameters of the above signal model are unknown, thus deciding $\mathcal{H}_1$ if

$$\Lambda[n_0] = \frac{p(\boldsymbol{\varphi}_1[n_0], \ldots, \boldsymbol{\varphi}_L[n_0]; \hat{\boldsymbol{\theta}}_1[n_0], \mathcal{H}_1)}{p(\boldsymbol{\varphi}_1[n_0], \ldots, \boldsymbol{\varphi}_L[n_0]; \hat{\boldsymbol{\theta}}_0[n_0], \mathcal{H}_0)} > \gamma. \tag{6}$$

The N observations at time n_0 of lead l define the vector $\boldsymbol{\varphi}_l[n_0] = [\varphi_l[n_0], \ldots, \varphi_l[n_0 + N - 1]]^T$, $l = 1, \ldots, L$, and γ denotes the detection threshold. Under $\mathcal{H}_0$ and $\mathcal{H}_1$, the maximum likelihood (ML) estimates of the statistical parameters are defined by the vectors

$$\hat{\boldsymbol{\theta}}_0[n_0] = \begin{bmatrix} \hat{m}_{1,0}[n_0] \\ \vdots \\ \hat{m}_{L,0}[n_0] \end{bmatrix}, \quad \hat{\boldsymbol{\theta}}_1[n_0] = \begin{bmatrix} \hat{a}_1[n_0] \\ \vdots \\ \hat{a}_L[n_0] \\ \hat{m}_{1,1}[n_0] \\ \vdots \\ \hat{m}_{L,1}[n_0] \end{bmatrix}, \tag{7}$$

respectively. Hence, the GLRT is computed for each n_0, once $\hat{\boldsymbol{\theta}}_0[n_0]$ and $\hat{\boldsymbol{\theta}}_1[n_0]$ have been determined as described below. σ_l may be estimated in the same way as the other statistical parameters, i.e., for every n_0. However, in this case, $\hat{\sigma}_l$ is independently determined from an interval at the onset of the recording assumed not to contain any BPC. The resulting estimate is then held fixed during the remaining part of the recording, and employed under both $\mathcal{H}_0$ and $\mathcal{H}_1$.

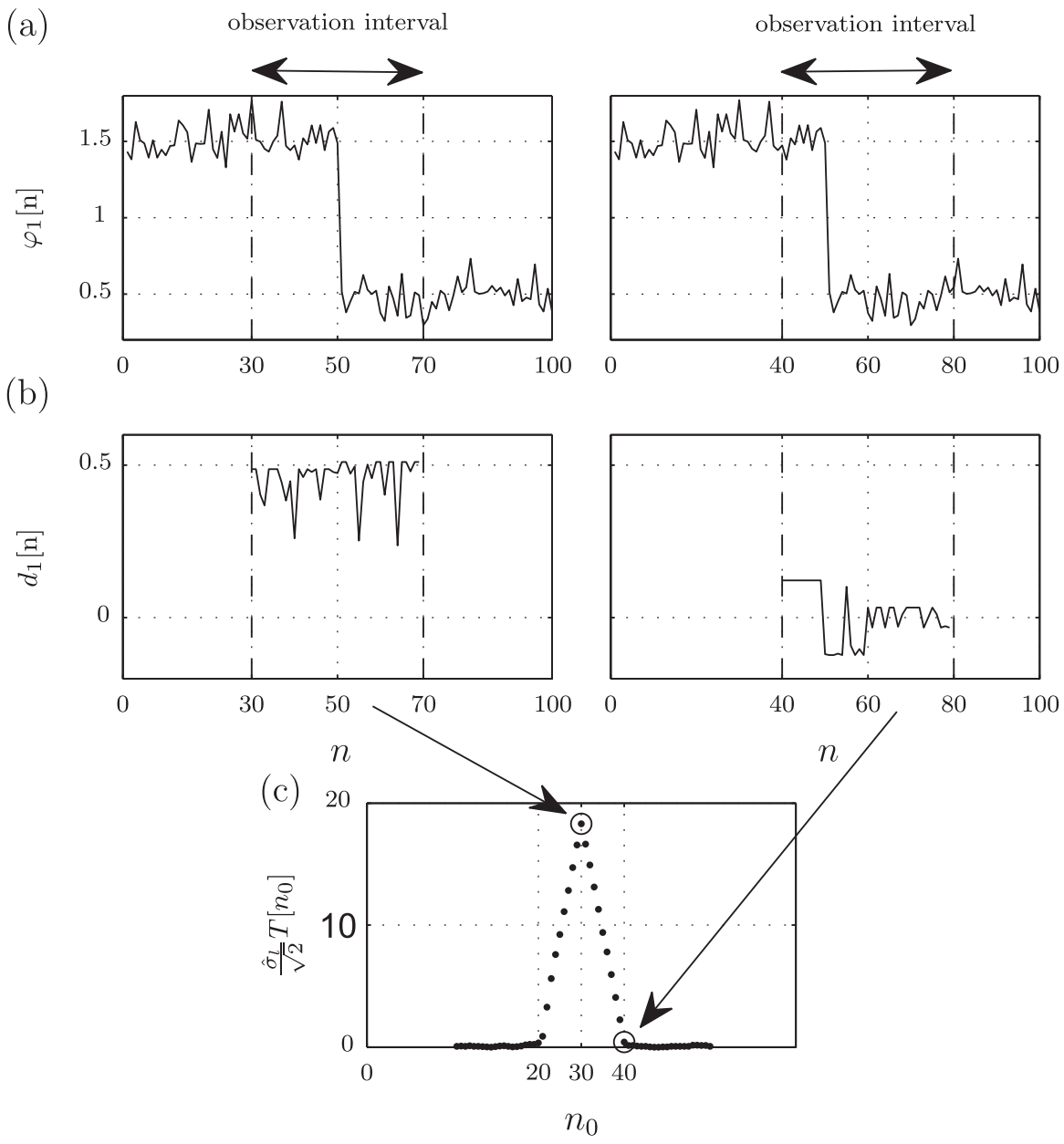

Fig. 2. Illustration of BPC detection with simulated observations $\varphi_1[n]$, produced by the model parameter values $L=1$, $N=40$, $a=0.5$, $m_1=1$, $\sigma_1=0.1$. (a) The distance function $\varphi_1[n]$ and two locations of the sliding observation interval, starting either at $n_0=0$ (left panel) or 5 (right panel). Since the BPC occurs at $n=20$, the observation interval of the left panel is centered over the BPC. (b) The distance function $d_1[n]$, defined in (9), displayed for the two observation intervals; the interpretation of $d_l[n]$ is given in the running text. (c) The detector output $T[n_0]$ with the output samples of the two observation intervals are encircled (corrected with respect to the delay $N/2=20$).

Inserting the Laplacian PDF in (6) and taking the logarithm of both sides, the detector output, defined by the left hand side of the GLRT, becomes

$$T[n_0] \stackrel{\text{def}}{=} \ln \Lambda[n_0] = \sum_{l=1}^{L} \frac{\sqrt{2}}{\hat{\sigma}_l} \sum_{n=n_0}^{n_0+N-1} d_l[n], \tag{8}$$

where

$$d_l[n] = |\varphi_l[n] - \hat{m}_{l,0}[n_0]| - |\varphi_l[n] - \hat{m}_{l,1}[n_0] - \hat{a}_l[n_0]s[n-n_0]|. \tag{9}$$

The detector output $T[n_0]$ can be interpreted as a distance between the signal amplitude a_l and the standard deviation σ_l of the noise. This can be realized by noticing that, under $\mathcal{H}_1$, the first term $|\varphi_l[n] - \hat{m}_{l,0}[n_0]|$ in (9) can be viewed as an estimate of the signal amplitude, whereas the second term $|\varphi_l[n] - \hat{m}_{l,1}[n_0] - \hat{a}_l[n_0]s[n-n_0]|$ can be viewed as an estimate of the residual noise. Note that $T[n_0]$ includes the information of all the leads.

The computation of the detection function $T[n_0]$ is illustrated in Fig. 2 for a simulated signal where the occurrence time of the BPC is known.

In order to account for information which derive from both the QRS complex and the ST–T segment, the total detector output $\mathcal{T}[n_0]$ is obtained as a weighted sum [6]:

$$\mathcal{T}[n_0] = \lambda_{\text{QRS}} T_{\text{QRS}}[n_0] + \lambda_{\text{STT}} T_{\text{STT}}[n_0] > \gamma', \tag{10}$$

where $0 < \{\lambda_{\text{QRS}}, \lambda_{\text{STT}}\} < 1$, $\lambda_{\text{QRS}} + \lambda_{\text{STT}} = 1$, and the threshold $\gamma' = \ln \gamma$. Since a sliding observation interval is analyzed, several peaks of $\mathcal{T}[n_0]$ will exceed γ' when a BPC occurs, see Fig. 3. In order to avoid detection of very gradual transitions, resulting in very wide peaks, the width must be within the interval $[W_{\min}, W_{\max}]$. Width is here defined by the time that elapses between two successive

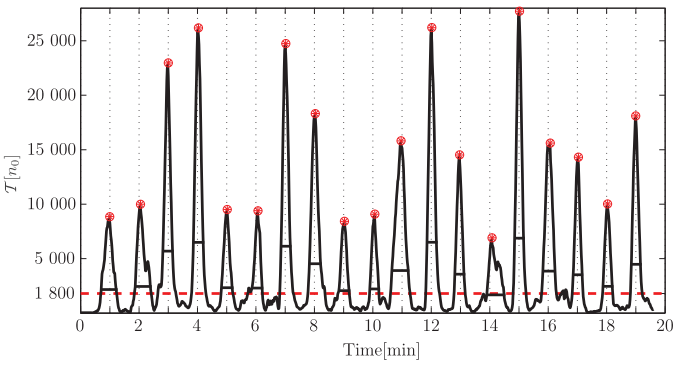

Fig. 3. GLRT-based detector output $\mathcal{T}[n_0]$ for a subject changing body position every minute. The threshold γ' is set to 1800 (dashed line). Peak width is indicated, determined at 25% of the peak amplitude.

crossings at the 25% level of the peak amplitude of $\mathcal{T}[n_0]$. The lower limit $W_{\min}$ avoids detection of noise bursts, whereas the upper limit $W_{\max}$ avoids detection of ischemic episodes. For peaks with acceptable width, the time for the maximal value of $\mathcal{T}[n_0]$ defines the occurrence time of a BPC. A 10-s refractory period is applied after each detection [6]. A BPC is almost invariably accompanied with a temporary reduction in SNR. This property can be explored for the purpose of rejecting falsely detected BPCs with a test that checks the SNR of beats that surround a preliminary detection. The following simple test is employed: a BPC is detected when the average SNR of a surrounding 20-beat interval is below a fixed threshold (excessively noisy beats have already been rejected by preprocessing). If the test is not fulfilled, the preliminary detection is most likely caused by an ischemic episode and therefore rejected.

2.4. ML estimation of statistical parameters

The ML estimators of $m_{l,0}[n_0]$, $m_{l,1}[n_0]$, and $a_l[n_0]$ are given by (see Section 4):

$$\hat{m}_{l,0}[n_0] = \text{median}\{\varphi_l[n]\}, \tag{11}$$

$$\hat{m}_{l,1}[n_0] = \text{median}\{\varphi_l[n] - \hat{a}_l[n_0]s[n-n_0]\}, \tag{12}$$

$$\hat{a}_l[n_0] = \text{median}\{(\varphi_l[n] - \hat{m}_{l,1}[n_0])s[n-n_0]\}, \tag{13}$$

respectively, for $n = n_0, \ldots, n_0 + N - 1$. The counterparts of these ML estimators under the Gaussian assumption are quite straightforward to derive by substituting the PDF in (5), resulting in: $\hat{m}_{l,0}[n_0] = \hat{m}_{l,1}[n_0] = \text{mean}\{\varphi_l[n]\}$ and $\hat{a}_l[n_0] = \text{mean}\{\varphi_l[n]s[n-n_0]\}$, and not requiring any optimization procedure.

Since $\hat{m}_{l,1}[n_0]$ and $\hat{a}_l[n_0]$ depend on each other, alternating optimization is introduced. In order to have an initial estimate of $m_{l,1}|n_0]$, an interpretation of the PDF of the noise $w_l[n]$ under $\mathcal{H}_1$, which may be expressed as

$$w_l[n] = \varphi_l[n] - a_l[n_0]s[n-n_0], \tag{14}$$

is helpful. Under $\mathcal{H}_1$, the PDF of $\varphi_l[n]$ is given by two Laplacian PDFs shifted by either $+a_l[n_0]$ or $-a_l[n_0]$ due to the definition of the step function $s[n]$ in (4), see Fig. 4. Analogously, the PDF of $w_l[n]$ in (14) can be interpreted as the PDF of the first half of $\varphi_l[n]$, shifted $-a_l[n_0]$, superimposed with second half of $\varphi_l[n]$, shifted $+a_l[n_0]$, see Fig. 4(a). By comparing the two PDFs, it is noted that the median of $w_l[n]$ in (14) can be replaced by the median of $\varphi_l[n]$ since no knowledge of $a_l[n_0]$ is required. The replacement to estimate $m_{l,1}[n_0]$ in Fig. 4(b) suffers from the limitation that the PDF of $\varphi_l[n]$ has few data at $m_{l,1}[n_0]$, which thus may cause a significant error when computing the median. Therefore, the median of $\varphi_l[n]$ is proposed as an initial estimate of $m_{l,1}[n_0]$, introduced in (13) to find $\hat{a}_l[n_0]$, then inserted in (12), and so on until convergence. Here, convergence is judged to

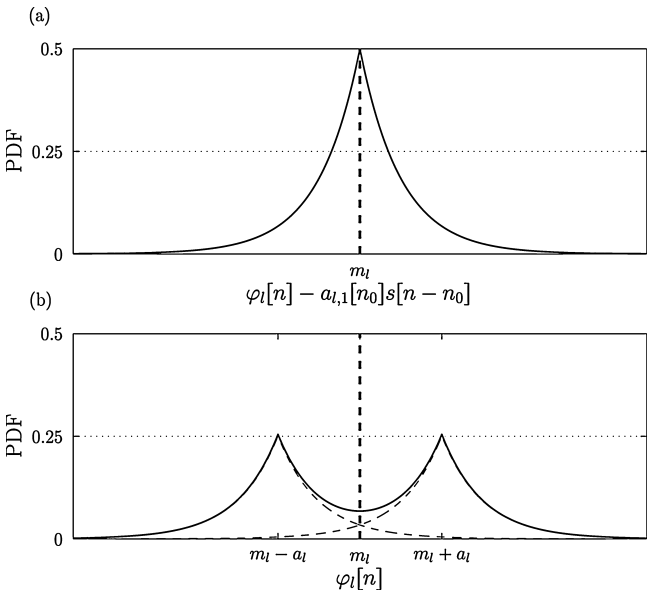

Fig. 4. (a) The PDF of $\varphi_l[n] - a_{l,1}[n_0]s[n-n_0]$, and (b) the PDF of $\varphi_l[n]$, both displayed for hypothesis $\mathcal{H}_1$. Note that the index n_0 has been suppressed for the locations $m_l - a_l$, m_l, $m_l + a_l$ for reasons of legibility.

be reached when $\hat{m}_{l,1}[n_0]$ and $\hat{a}_l[n_0]$ reach stable values, typically requiring less than 10 iterations.

The standard deviation σ_l of the Laplacian PDF[1] is determined from an interval with N_σ samples located at the onset of $\varphi_l[n]$, i.e., $n_0 = 0$, using the ML estimator [18]:

$$\hat{\sigma}_l = \frac{\sqrt{2}}{N_\sigma}\sum_{n=0}^{N_\sigma - 1}|\varphi_l[n] - \hat{m}_{l,0}[0]|. \tag{15}$$

3. Materials

The performance of the GLRT-based detector was evaluated on two databases: one with healthy subjects performing BPCs to assess the detector performance in terms of sensitivity and positive predictivity value, and another from patients with induced ischemia to assess specificity by setting the probability of false alarm. In both cases, the standard 12-lead ECG was acquired at a sampling rate of 1 kHz and an amplitude resolution of 0.6 μV.

The BPC database consists of 20 healthy subjects who performed BPCs according to the following protocol: supine-to-right side, supine-to-left side, supine-to-right side, and so on. The complete sequence was repeated five times with a 1-min duration of each BPC, for details, see [7].

The STAFF III database consists of 83 patients subjected to elective prolonged balloon occlusion during PTCA, using balloon catheters for occlusion in one of the major coronary arteries [17,19]. Since it is highly unlikely that the patient changes body position during PTCA, it is assumed that no BPCs occur in this database [7].

The choice of noise model is investigated on the BPC database by comparing the likelihood function related to Laplacian noise,

$$L_L(\sigma_L; \mathbf{x}_l) = \prod_{n\in\Omega}\frac{1}{\sqrt{2\sigma_L^2}}\exp\left[-\frac{\sqrt{2}}{\sigma_L}|\tilde{\varphi}_l[n]|\right], \tag{16}$$

[1] The Gaussian counterpart of the standard deviation is $\hat{\sigma}_l^2 = \frac{1}{N_\sigma}\sum_{n=0}^{N_\sigma-1}(\varphi_l[n] - \hat{m}_{l,0}[0])^2$.

to the one related to Gaussian noise,

$$L_G(\sigma_G;\mathbf{x}_l)=\prod_{n\in\Omega}\frac{1}{\sqrt{2\pi\sigma_G^2}}\exp\left[-\frac{\tilde{\varphi}_l^2[n]}{2\sigma_G^2}\right]. \tag{17}$$

For each patient, $L_L(\sigma_L;\mathbf{x}_l)$ and $L_G(\sigma_G;\mathbf{x}_l)$ are evaluated for all samples located in the intervals in between BPCs ("the noise samples"), denoted $\tilde{\varphi}_l[n]$. Together these samples define the set Ω. The notation $\tilde{\varphi}_l[n]$ indicates that the median, computed from each segment in each lead, has been subtracted from $\varphi_l[n]$; the mean has instead been subtracted when the Gaussian model is studied.

Detector performance is evaluated on the BPC database using probability of detection P_D and probability of false alarm P_F. These two probabilities are estimated from the number of true detections (N_T), false alarms (N_F), and missed detections (N_M) such that:

$$P_D=\frac{N_T}{N_T+N_M}, \tag{18}$$

$$P_F=\frac{N_F}{N_T+N_F}. \tag{19}$$

Since no BPCs are assumed to occur in the STAFF III database, the false alarm rate R_F is employed as performance measure, defined as the number of false BPCs per hour [6]. The false alarm rate R_F was set by tuning γ' on the STAFF III database, after which the resulting γ' was used to evaluate performance on the BPC database in terms of P_F and P_D.

4. Calculation

The computation of the GLRT in (8) requires that the three ML estimators $\hat{m}_{l,0}$, $\hat{m}_{l,1}$, and $\hat{a}_{l,1}$ have been determined – an issue which is addressed in this section. When hypothesis $\mathcal{H}_0$ is assumed, $\hat{m}_{l,0}$ is found by maximizing the related log-likelihood function with respect to $m_{l,0}$, i.e.,

$$\hat{m}_{l,0}=arg\ \max_{m_{l,0}}\ \ln p(\boldsymbol{\varphi}_l;m_{l,0}). \tag{20}$$

Inserting the Laplacian noise model, it is easily shown that the maximization in (20) is equivalent to minimizing the cost function:

$$J_0(m_{l,0})=\sum_{n=n_0}^{n_0+N-1}|\varphi_l[n]-m_{l,0}|. \tag{21}$$

Its minimum is reached when $m_{l,0}$ is equal to the median of the observed data, and thus

$$\hat{m}_{l,0}=\text{median}\{\varphi_l[n]\} \tag{22}$$

for $n=n_0,\ldots,n_0+N-1$.

Assuming instead hypothesis $\mathcal{H}_1$, the ML estimators of $m_{l,1}$ and $a_{l,1}$ are determined from

$$[\hat{m}_{l,1},\hat{a}_{l,1}]=arg\max_{m_{l,1},a_{l,1}}\ln p(\boldsymbol{\varphi}_l;m_{l,1},a_{l,1}), \tag{23}$$

being equivalent to minimizing the cost function,

$$J_1(m_{l,1},a_{l,1})=\sum_{n=n_0}^{n_0+N-1}|\varphi_l[n]-m_{l,1}-a_{l,1}\ \ s[n-n_0]|, \tag{24}$$

with respect to $m_{l,1}$ and $a_{l,1}$. The partial derivative of $J_1(m_{l,1},a_{l,1})$ with respect to $m_{l,1}$ equals

$$\frac{\partial J_1(m_{l,1},a_{l,1})}{\partial m_{l,1}}=-\sum_{n=n_0}^{n_0+N-1}\text{sgn}(\varphi_l[n]-m_{l,1}-a_{l,1}\,s[n-n_0]), \tag{25}$$

which, when set to zero, yields the MLestimator,

$$\hat{m}_{l,1}=\text{median}\{\varphi_l[n]-a_{l,1}\ \ s[n-n_0]\} \tag{26}$$

for $n=n_0,\ldots,n_0+N-1$.

The partial derivative of $J_1(m_{l,1},a_{l,1})$ with respect to $a_{l,1}$ equals

$$\frac{\partial J_1(m_{l,1},a_{l,1})}{\partial a_{l,1}}=-\sum_{n=n_0}^{n_0+N-1}s[n-n_0]\text{sgn}(\varphi_l[n]-m_{l,1}-a_{l,1}s[n-n_0]). \tag{27}$$

Inserting the definition of $s(n)$, cf. (4), this expression becomes

$$\frac{\partial J_1(m_{l,1},a_{l,1})}{\partial a_{l,1}}=-\sum_{n=n_0}^{n_0+N/2-1}\text{sgn}(\varphi_l[n]-m_{l,1}-a_{l,1})+\sum_{n=n_0+N/2}^{n_0+N-1}\text{sgn}(\varphi_l[n]-m_{l,1}+a_{l,1}), \tag{28}$$

which in turn can be rewritten as

$$\begin{aligned}\frac{\partial J_1(m_{l,1},a_{l,1})}{\partial a_{l,1}}&=-\sum_{n=n_0}^{n_0+N/2-1}\text{sgn}(\varphi_l[n]-m_{l,1}-a_{l,1})\\&\quad-\sum_{n=n_0+N/2}^{n_0+N-1}sgn(-\varphi_l[n]+m_{l,1}-a_{l,1})\\&=-\sum_{n=n_0}^{n_0+N-1}sgn((\varphi_l[n]-m_{l,1})s[n-n_0]-a_{l,1}).\end{aligned} \tag{29}$$

Consequently, the ML estimator of $a_{l,1}$ is given by

$$\hat{a}_{l,1}=\text{median}\{(\varphi_l[n]-m_{l,1})\ \ s[n-n_0]\} \tag{30}$$

for $n=n_0,\ldots,n_0+N-1$. It should be noted that the ML estimators of $m_{l,1}$ and $a_{l,1}$ depend on each other, and therefore an alternating optimization algorithm is employed.

5. Results

The following parameter setup was used when evaluating detector performance: $\lambda_{QRS}=0.8$, $N=44$ s, $N_\sigma=50$ s, $W_{\min}=15$ s, $W_{\max}=50$ s, $K=4$, and $\gamma'=1800$.

The histogram of the noise samples $\tilde{\varphi}_l[n]$, resulting from the subjects of the BPC database, is displayed in Fig. 5. The preprocessing makes it permissible to merge all the data after subtracting the median, and the resulting histogram may also be relevant for individual subjects. The shape of the histogram suggests that the Laplacian PDF is better as a noise model than the Gaussian one.

Focusing on each subject-specific histogram, the maximum value of the log-likelihood function $L_L(\sigma_L;\mathbf{x}_l)$ in (16) is displayed versus the maximum value of the log-likelihood function $L_G(\sigma_G;\mathbf{x}_l)$ in (17) for both the QRS complex and the ST–T segment of lead X, see Fig. 6. Leads Y and Z are not displayed since their histograms are similar to that of lead X. The results in Fig. 6 suggest that the noise is better modeled by a Laplacian PDF than from a Gaussian PDF since all displayed points are below the diagonal.

Fig. 7 presents, as a function of γ', the performance on the BPC database in terms of P_D and P_F, and the performance on the STAFF III database in terms of false alarm rate R_{FA}. The false alarm rate at $\gamma'=1800$ was used to determine the performance of the present BPC detector.

The results presented in Table 1 show that the performance of the Bayesian detector based on the Gaussian noise model [6] is

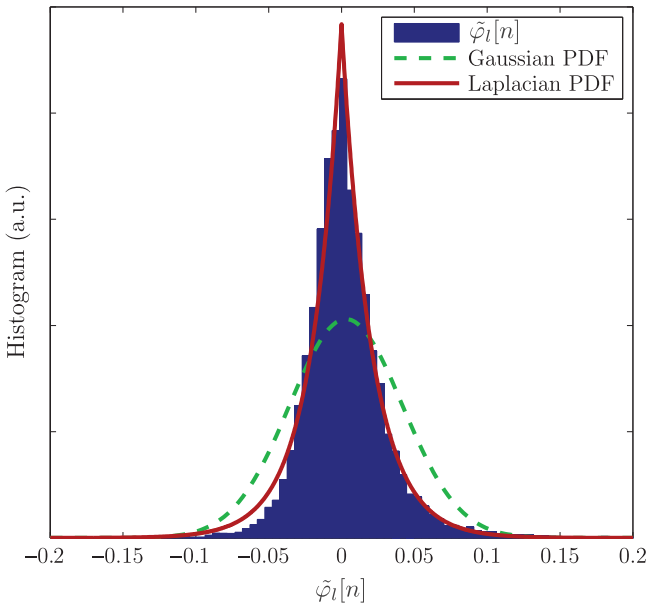

Fig. 5. The histogram of $\tilde{\varphi}_l(n)$, displayed together with the best fit of the Laplacian and Gaussian PDFs obtained by maximizing the respective likelihood functions.

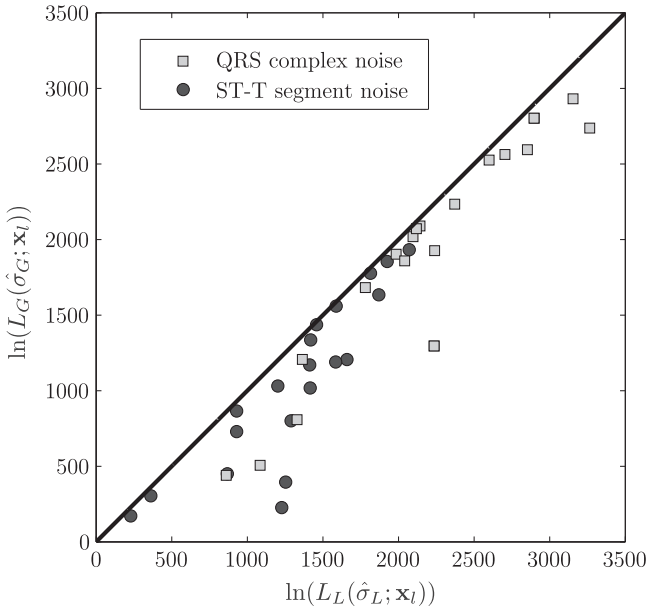

Fig. 6. The maximum value of the Laplacian log-likelihood function, i.e., $L_L(\hat{\sigma}_L;\mathbf{x}_l)$, is displayed versus the maximum value of the Gaussian log-likelihood function, i.e., $L_G(\hat{\sigma}_G;\mathbf{x}_l)$, for the subjects of the BPC database.

Table 1
Performance statistics for the BPC detection. The false alarm rate R_F is expressed as a mean and standard deviation.

Detector	BPC database P_D	P_F	STAFF III database R_F (events/h)
Laplacian-based	0.94	0.00	1 ± 3
Gaussian-based [6]	0.90	0.01	2 ± 7

clearly inferior to that of the present detector. Note that the values of R_F of the Laplacian detector have been rounded to the nearest integer in order to match the integer values reported on in that study.

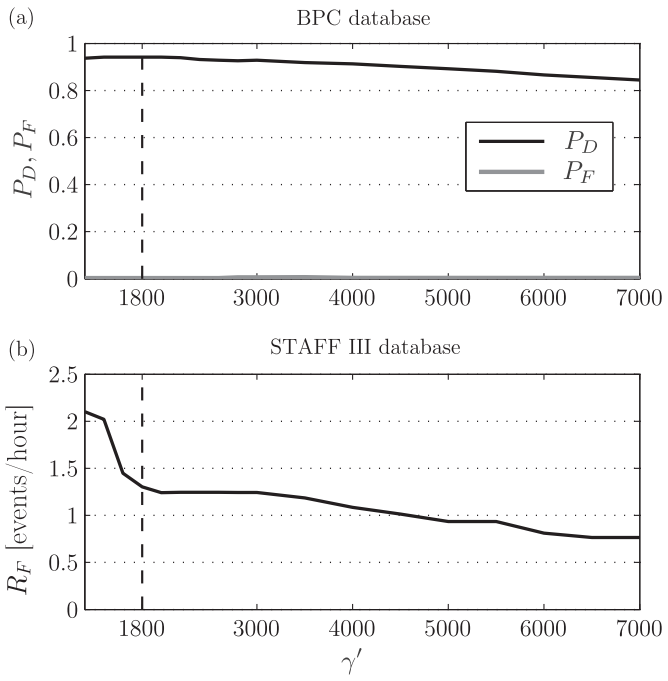

Fig. 7. Performance of the GLRT detector as a function of the threshold γ' on (a) the BPC database, and (b) the STAFF III database. The threshold $\gamma' = 1800$, used for computing the results in Table 1, is displayed with dashed line. Note that P_F coincides with the horizontal axis in (a) since it is identical to zero.

6. Discussion

This study shows that the Laplacian noise model is better for representing the impulsive nature of the noise observed in the KLT domain. This finding implies that there is no longer a need for robustifying ad hoc measures such as the median absolute deviation filter which was previously employed for the purpose of rejecting outliers in the detector based on the Gaussian noise model.

The present detector includes a test whose aim is to discard detections caused by ischemic episodes. Since such episodes are manifested by much wider peaks in $\mathcal{T}[n_0]$ than is a BPC, peak width is required not to exceed an upper limit. In other applications where the present detector may be of interest to use, the lower and upper limits of the width should be adjusted so that the degree of steepness of the change is well-matched. In addition to exploring peak width for detection, recent results suggest that exploration of differences in the respective KLT series of the QRS complex and the ST–T segment can improve discrimination of ischemic episodes from BPCs [8]; this feature was not explored in the present study.

The present BPC detector was initially tested for a fixed standard deviation σ_L. However, by estimating this parameter at the onset of the ECG recording, a 12% increase in P_D was achieved without any accompanying reduction in P_F. The alternating optimization was found to always converge within 10 iterations or less; no instabilities were observed for this type of optimization. Another approach to estimate $\hat{m}_{l,1}$ and $\hat{a}_{l,1}$ is based on the observation that the cost function in (24) can be treated as a least absolute deviation (LAD) regression problem, using an optimization algorithm such as the one presented in [20]. Instead of using the MLE, other estimators may be used. For example, when estimating the median as the average of the median of the first half and the second half of the data, $\hat{a}$ becomes:

$$\hat{a}_{l,\mathcal{H}_1} = \frac{median\{\varphi_l[n_0,\ldots,n_0+N/2\} - \text{median}\{\varphi_l[n_0+N/2+1,\ldots,n_0+N]\}}{2} \quad (31)$$

In simulated data, this heuristic estimator did not produce estimates that are significantly different from the MLE when analyzing signals with low SNR while in signals with higher SNR, the detection output peaks were slightly wider. This simpler estimator could be used as initialization of the iterative process.

The false alarm rates reported in Table 1 may seem rather high at a first glance. However, it is important to realize that occlusion during PTCA is complete and very fast, while unprovoked ischemic events have a much smoother transient signature in the KLT coefficient series of the QRS complex and ST–T segment. As a consequence, the false alarm rate is expected to be much lower when analyzing ambulatory recordings or during ST monitoring, both target contexts for the present BPC detector. A limitation of the present study is that BPCs are rather uniform in appearance and speed, whereas this may not be the case in real life where also changes from sitting to standing may occur.

The detection threshold γ' was determined so that a specific false alarm rate was obtained on the STAFF III database, after which the resulting threshold value was applied to the BPC database to evaluate the performance in terms of P_D and P_F. Division of the dataset into learning and test sets was not suitable since the available dataset is small. Instead, the present approach was adopted in which the threshold was first set for a database without BPCs and then evaluated on a database consisting of different types of BPCs.

In this work BPCs have been modelled as step-like functions. Other transient functions such as sigmoids were also considered. Whilst increasing mathematical complexity, they did not improved detection performance. Hence, the simpler step-like function has been retained.

We have evaluated the BPC detector in two complementary and rather extreme cases: one database with abrupt ischemic changes from a PCI procedure for specificity analysis, and another database with controlled BPCs for assessing sensitivity. For the STAFF III database, the complete artery occlusion may induce abrupt changes in the ST–T waveforms, which in turn, can be misclassified as BPC. Under less severe ischemic episodes, it is expected that the false alarm rate will be lower than that obtained in our case. For the BPC database, the postural changes are complete whereas a partial change could induce a less marked signature that would lead to lower sensitivity. However, this observation needs to be considered in view of that an incomplete BPC should still be detected as a BPC, possibly calling for further considerations on detector design.

The BPC detector may misclassify certain types of arrhythmias such as ventricular fibrillation, which modify severely QRS morphology. However, for an important increase in HR, such as during exercise, there are studies which have shown that the QRS duration remains largely unaltered as well as the magnitude and spatial orientation of the maximum QRS vectors [21,22]. Therefore, an increase in HR should not modify the QRS complex and, accordingly, the QRS KLT coefficient series. The ST–T waveform may be modified due to its dependence on HR, although it only contributes by 20% to the detector statistics, in comparison with the 80% of the QRS, so the expected influence on the BPC detector should be low. The potential influence of ST–T changes due to ischemia is already taken into account in the STAFF III database, which has been used to test the robustness of the detector to extreme ST–T changes.

The present GLRT-based detector can be used in other biomedical applications where it is of interest to detect abrupt changes in Laplacian noise, e.g., in the prediction of intradialytic hypotension which induces abrupt changes in the amplitude of the photoplethysmographic signal [10].

7. Conclusions

The problem of BPC detection was addressed by investigating a Laplacian noise model of the KLT coefficient series which characterize the QRS complex and the ST–T segment. The GLRT-based detector was derived, embracing the estimation of a time-varying BPC amplitude as well as the mean and standard deviation of the Laplacian noise. The noise in the KLT domain was found to be better characterized by the Laplacian noise model than the Gaussian one. Furthermore, the performance achieved by the GLRT-based detector was superior to that achieved by a previously published detector based on the Gaussian noise model, both with respect to sensitivity/specificity and false alarm rate. It is concluded that the proposed BPC detector improves the accuracy of ischemia monitoring.

Acknowledgements

AM is supported by a Marie Curie Intra-European Fellowship (FP7-PEOPLE-2011-IEF). This work was supported by the grants TEC2010-19410 and TEC2010-21703-C03-02 from MINECO, Spain, and by Grupo Consolidado GTC from DGA, Spain.

References

[1] T. Jernberg, B. Lindahl, M. Högberg, L. Wallentin, Effects on QRS waveforms and ST–T-segment by changes in body position during continuous 12-lead ECG: a preliminary report, in: Proceeding of Computers in Cardiology, IEEE Press, 1997, pp. 461–464.
[2] B.L. Nørgaard, B.M. Rasmussen, M. Dellborg, K. Thygesen, Positional changes of spatial QRS- and ST-segment variables in normal subjects: implications for continuous vectorcardiography monitoring during myocardial ischemia, J. Electrocardiol. 33 (1) (2000) 23–30.
[3] M.G. Adams, B.J. Drew, Body position effects on the ECG: implication for ischemia monitoring, J. Electrocardiol. 30 (4) (1997) 285–291.
[4] M. Satoh, W. Hida, T. Chonan, S. Okabe, H. Miki, O. Taguchi, Y. Kikuchi, T. Takishima, Effects of posture on carbon dioxide responsiveness in patients with obstructive sleep apnoea, Thorax 48 (1993) 537–541.
[5] F. Jager, R.G. Mark, G.B. Moody, S. Divjak, Analysis of transient ST segment changes during ambulatory monitoring using the Karhunen–Loève transform, in: Proceeding of Computers in Cardiology, IEEE Computer Society Press, 1992, pp. 691–694.
[6] J. García, M. Åström, J. Mendive, P. Laguna, L. Sörnmo, ECG-based detection of body position changes in ischemia monitoring, IEEE Trans. Biomed. Eng. 25 (6) (2003) 501–507.
[7] M. Åström, J. García, P. Laguna, O. Pahlm, L. Sörnmo, Detection of body position changes using the surface electrocardiogram, Med. Biol. Eng. Comput. 41 (2) (2003) 164–171.
[8] A. Mincholé, F. Jager, P. Laguna, Discrimination between ischemic and artifactual ST segment events in Holter recordings, Biomed. Signal Proc. Control 5 (1) (2010) 21–31.
[9] J.P. Martínez, S. Olmos, Methodological principles of T wave alternans analysis: a unified framework, IEEE Trans. Biomed. Eng. 52 (4) (2005) 599–613.
[10] K. Solem, B. Olde, L. Sörnmo, Prediction of intradialytic hypotension using photoplethysmography, IEEE Trans. Biomed. Eng. 57 (7) (2010) 1611–1619.
[11] P.-H. Niemenlehto, M. Juhola, Detection of saccadic eye movements using the order statistic constant false alarm rate technique, in: Proceeding of the IASTED International Conference on Biomedical Engineering (BIOMED), ACTA Press Anaheim, 2008, pp. 29–33.
[12] T. Pander, An application of robust filters in ECG signal processing, J. Med. Inform. Technol. 10 (2006) 113–124.
[13] H. Rabbani, A fast method for despeckling in wavelet domain using Laplacian prior and Rayleigh noise, in: Proceeding of the International Conference on Information Technology and Applications in Biomedicine (ITAB), 2008, pp. 374–377.
[14] L. Edenbrandt, O. Pahlm, Vectorcardiogram synthesized from a 12-lead ECG: superiority of the inverse Dower matrix, J. Electrocardiol. 21 (4) (1988) 361–367.
[15] F. Badilini, W. Zareba, E. Titlebaum, A. Moss, Analysis of ST segment variability in Holter recordings, in: Noninvasive Electrocardiology: Clinical Aspects of Holter Monitoring. Frontiers in Cardiology, Saunders, London, U.K., 1996, pp. 357–372.
[16] P. Laguna, G. Moody, J. García, A. Goldberger, R. Mark, Analysis of the ST–T complex of the electrocardiogram using the Karhunen–Loève transform: adaptive monitoring and alternans detection, Med. Biol. Eng. Comput. 37 (1999) 175–189.
[17] J. García, P. Lander, L. Sörnmo, S. Olmos, G. Wagner, P. Laguna, Comparative study of local and Karhunen–Loève-based ST–T indexes in recordings from human subjects with induced myocardial ischemia, Comput. Biomed. Res. 31 (4) (1998) 271–292.

[18] S.M. Kay, Fundamentals of Statistical Signal Processing: Estimation Theory, Prentice Hall, New Jersey, 1993.
[19] J. Pettersson, E. Carro, L. Edenbrandt, O. Pahlm, M. Ringborn, L. Sörnmo, G. Wagner, S. Warren, Changes in high frequency QRS components are more sensitive than ST segment deviations for detecting acute coronary artery occlusion, J. Am. Coll. Cardiol. 36 (2000) 1827–1834.
[20] Y. Li, G.R. Arce, A maximum likelihood approach to least absolute deviation regression, J. Appl. Signal Proc. 12 (2004) 1762–1769.
[21] M. Simoons, P. Hugenholtz, Gradual changes of ECG waveform during and after exercise in normal subjects, Circulation 52 (4) (1975) 570–577.
[22] J. Deckers, R. Vinke, J. Vos, M. Simoons, Changes in the electrocardiographic response to exercise in healthy women, Br. Heart J. 64 (6) (1990) 376–380.